# Modeling of Diesel Spray Impingement on a Flat Wall

**Seong Hyuk Lee, Hong Sun Ryou***

*Department of Mechanical Engineering, Chung-Ang University*

To understand the transient behavior of droplets after impingement in a diesel engine, a numerical model for diesel sprays impinging on a flat wall is newly developed by the proposition of several mathematical formulae to determine the post-impingement characteristics of droplets. The new model consists of three representative regimes such as rebound, deposition and splash. The gas phase is modeled in terms of the Eulerian conservation equations, and the dispersed phase is calculated using a discrete droplet model. To validate the new model, the calculated results are compared with several experimental data. The results show that the new model is generally in good agreement with the experimental data. Therefore, it is thought that the new model is acceptable for the prediction of transient behavior of wall sprays.

**Key Words :** Diesel Engines, Sprays, Impingement, Rebound, Deposition, Splash

## Nomenclature

| | |
|---|---|
| $D$ | : Droplet diameter |
| $d_{sp}$ | : Diameter of the spread film disc |
| $m$ | : Droplet mass |
| $N$ | : Number of droplets in a parcel |
| $Oh$ | : Ohnesorge number |
| $Re$ | : Reynolds number |
| $u_g, v_g, w_g$ | : Velocity component of the gas phase |
| $u'_g, v'_g, w'_g$ | : Fluctuating velocity component of the gas phase |
| $u_d, v_d, w_d$ | : Velocity component of the dispersed phase |
| $V$ | : Total velocity of droplet or control volume |
| $v_t, v_n$ | : Tangential and normal components of droplet velocity, respectively |
| $We^T$ | : Weber number based on the total droplet velocity |
| $We_n$ | : Weber number based on the normal droplet velocity |
| $\Theta_i$ | : Incident angle of impinging droplets measured from the wall |
| $\theta$ | : Void fraction |
| $\mu$ | : Viscosity |
| $\rho$ | : Density of the gas phase |
| $\sigma$ | : Surface tension |
| $\varPhi$ | : Viscous dissipated energy of liquid film built on the wall |
| $\varPsi$ | : Time fraction at which the splash occurs |
| $\forall_f$ | : Volume of the film disc |

**Subscripts**

| | |
|---|---|
| $a, b$ | : After and before impingement, respectively |
| $d$ | : Droplet |
| $f$ | : Film |
| rel | : Relative |
| $w$ | : Wall surfaces |

* Corresponding Author,
  E-mail : cfdmec@cau.ac.kr
  TEL : +82-2-820-5280 ; FAX : +82-2-814-9476
  Professor, Department of Mechanical Engineering, Chung-Ang University, HeukSuk Dong, DongJak Ku, Seoul 156-756, Korea. (Manuscript **Received** August 16, 1999; **Revised** March 16, 2000)

## 1. Introduction

The impingement of spray droplets on solid surfaces is a well-known phenomenon encountered in nature and technical applications. In particular, the spray impingement is very important in the application of small direct injection(DI) diesel engines where sprays impinge on the piston walls unavoidably. During cold starting, as

pointed out by Gonzalez et al. (1991), the low gas pressure facilitates spray penetration and forms the fuel-rich zones close to the wall surface, leading to incomplete combustion with consequently high levels of unburned hydrocarbons and soot particles in the exhaust gases. Therefore, it is necessary to clarify the characteristics of the spray/wall interaction in order to design the more efficient engines and to reduce the emissions.

A number of numerical sub-models for the spray impingement have been developed for describing the interaction between droplets and the wall. Naber and Reitz(1988) have developed a model to study spray impingement using the KIVA code. The main weakness in this model is to ignore the phenomenon of droplet shattering occurring at high collision energy and the loss of momentum and energy of the impinging droplets. Among earlier published models to complement the weakness of the above model, there are several models proposed by Watkins and Wang(1993), Guerrassi and Champoussin(1996), Eckhause and Reitz(1995) and Park(1994). These models were intrinsically based on the same experimental background as the Naber and Reitz's model (1988). In other words, these models described the transition criterion between the rebound and wall jet regimes by using the experimental data from Wachters and Westerling(1966) on a very hot wall whose temperature was above the Leidenfrost temperature of the fuel. However, the regime criterion used in the above models may not be applicable to a wall whose temperature is below the fuel boiling temperature because the appropriate hydrodynamic regime to a cold starting situation in DI diesel engines is the evaporative wetting regime as suggested by Eckhause and Reitz(1995), Senda et al. (1997) and Naber and Farrell(1993). Therefore, it is difficult to reasonably describe the splash phenomenon that occurs in a typical cold starting situation. Actually, the interaction between the liquid film deposited on the wall and impinging droplets is important in a typically cold start situation of DI engine, resulting in the splash phenomena. Consequently, the results of these models under-predicted significantly the dispersion of sprays away

from the wall due to the relatively simple modeling of the re-atomization with respect to the diameter and velocity of the ejected droplets. In other words, it may be concluded that these models can not effectively describe the splash phenomenon, which typically occurs in direct injection diesel engines because there are basically insufficient physical bases on splash mechanism in these models. As efforts to complement these weaknesses, Bai and Gosman(1995), Stanton and Rutland(1996), Mundo et al. (1998) and Senda et al. (1997) have proposed the impingement model and showed the improved results for several test cases.

The aim of the present study is to propose a new spray-wall interaction model for the non-evaporative sprays impinging on the cold and wetted wall. The 'cold wall' means one with the temperature below the fuel boiling point. The new model was devised in a different way from the earlier published models(Bai and Gosman, 1995; Stanton and Rutland, 1996; Mundo et al., 1998; Senda et al., 1997). The main difference between the new model and the above models is in the determination of tangential droplet velocity and ejection angle. The new model uses a theoretical relationship to represent the dissipated energy of liquid film built on the wall, instead of using the experimental correlation. By using the relationship, the total Weber number of ejected droplets can be determined from the energy conservation law, and the dissipated energy of droplets is described as a function of droplet Reynolds and Weber numbers. To assess the new model, numerical simulations were carried out for the non-evaporative sprays impinging on the wall and the predictions using the new model were compared with the several sources of experimental data.

## 2. Governing Equations

### 2.1 CFD models of the continuous and dispersed phase

For gas-phase, Eulerian partial differential equations are solved for the conservation of mass and momentum and for the modified k-$\varepsilon$ model proposed by Reynolds(1980), and can be written

using a cartesian coordinate in the general form:

$$\frac{1}{\Delta V}\frac{\partial}{\partial t}(\theta\rho\Delta V\phi)+\frac{\partial}{\partial x}(\theta\rho u_g\phi)$$

$$+\frac{\partial}{\partial y}(\theta\rho v_g\phi)+\frac{\partial}{\partial z}(\theta\rho w_g\phi)$$

$$=\frac{\partial}{\partial x}(\theta\Gamma_\phi\frac{\partial\phi}{\partial x})+\frac{\partial}{\partial y}(\theta\Gamma_\phi\frac{\partial\phi}{\partial y})$$

$$+\frac{\partial}{\partial z}(\theta\Gamma_\phi\frac{\partial\phi}{\partial z})+S_\phi+S_\phi^d \qquad (1)$$

where $\Delta V$ is the local incremental volume, $\rho$ denotes the density of the gas-phase, $\phi$ represents momentum, mass, fuel vapor fraction, turbulent kinetic energy, dissipation energy and specific energy, and $\theta$ is the void fraction, indicating the volume fraction occupied by the gas. The $\Gamma_\phi$ and $S_\phi$ are the diffusion coefficient and source terms of $\phi$. The source terms with subscript d come from interactions with the liquid phase. The liquid-phase is modeled in a stochastic manner as a spray of discrete droplets, which can penetrate and interact with the gas-phase. The droplet trajectory and momentum equations are written in terms of the droplet positions as follows:

$$\frac{dx_d}{dt}=u_d, \ \frac{dy_d}{dt}=v_d, \ \frac{dz_d}{dt}=w_d \qquad (2)$$

$$\frac{du_d}{dt}=K_d(u_g+u_g'-u_d)+S_{ud} \qquad (3a)$$

$$\frac{dv_d}{dt}=K_d(v_g+v_g'-v_d)+S_{vd} \qquad (3b)$$

$$\frac{dw_d}{dt}=K_d(w_g+w_g'-w_d)+S_{wd} \qquad (3c)$$

The coefficient $K_d$ is given by

$$K_d=\frac{3}{4}C_D\frac{\rho}{\rho_d}\frac{1}{D_d}V_{rel} \qquad (4)$$

where all the effects on the droplet of shear and pressure gradients are assumed to be absorbed in the coefficient $K_d$ and $C_D$ denotes the drag coefficient.

### 2.2 New impingement model

The main features of the new model are in the usage of regime criteria based on the consistent experimental results, in the determination of the post-impingement characteristics based on the energy conservation law and experimental results, and in the methodology on the transient behavior of film built on the wall. According to Kolpakov

et al. (1985), the collision of a droplet with liquid surface, where the wall temperature is less than the liquid boiling temperature, may result in sticking, rebounding, spreading, or splashing. In the present study, the stick region is ignored on the wetted wall because this regime occurs typically at very low impact energy. Hence, there are three regimes such as rebound, deposition and splash in the new model.

Prior to the model development, the regime criterion should be determined. The rebound regime occurs when a impinging droplet bounces off the film when the impact energy is low. The transition criterion between deposition and rebound is given as Weber number of 5 from the work of Bai and Gosman(1995). In the rebound regime where Weber number of an incident droplet is smaller than 5, the velocity of a rebounding droplet is determined by using the method developed by Matsumoto and Saito(1970) for small particles bouncing on a wetted surface, as follows:

$$v_{at}=5v_{bt}/7 \qquad (5)$$

$$v_{an}=-ev_{bn} \qquad (6)$$

where, $e$ is given by the following relationship.

$$e=0.993-1.76\Theta_i+1.56\Theta_i^2-0.49\Theta_i^3 \qquad (7)$$

where $\Theta_i$ represents the incident angle of impinging droplets measured from the wall surface. Mundo et al. (1995) have investigated multi-droplet impingement on rough surfaces and found the criterion between the deposition and splash regime. In the new model, the deposition-splashing boundary is determined by using the empirical correlation proposed by Mundo et al. (1995) as follows:

$$K=Oh \ Re_{bn}^{1.25}=57.7 \qquad (8)$$

where K is dimensionless parameter for impingement, expressed in terms of Reynolds and Ohnesorge numbers which are defined as $\rho_d D_b v_{bn}/\mu_d$ and $\mu_d/\sqrt{\rho_d\sigma_d D_d}$, respectively. For the formulation of splashing drop behavior, the first step is to determine the mass of the splashed drops. In order to describe the partial deposition and film existing at the wall, the ratio of the splashed mass to the mass of incident droplet is determined for a wetted surface by using the work of Bai and

Gosman (1995) as follows:

$$r_m = \frac{m_a}{m_b} = 0.2 + 0.9 RN(0, 1) \qquad (9)$$

where $RN(0, 1)$ is a random number distributed uniformly between 0 and 1. In the splash regime, the secondary drop size and the number of ejected drops are determined as follows:

$$D_a = C_w D_b \qquad (10)$$
$$N_{eject} = 0.187 \; We_{bn} - 4.45 \qquad (11)$$

where $C_w$ is given by $(r_m/N_{eject})^{1/3}$ from the mass conservation law. The number of ejected drops in a parcel can be given from the experimental data of Naber and Farrell (1993). Secondary velocity component of splashed droplets can be determined from the energy conservation law as follows:

$$0.5 m_b V_b{}^2 + \pi \sigma_d D_b{}^2 - \int_0^{t_e} \int_{\forall_f} \varPhi d \forall_f dt$$
$$= 0.5 m_a V_a{}^2 + \pi \sigma_d D_a{}^2 N_{eject} \qquad (12)$$

where $\forall_f$ is the volume of the fluid when the droplet is flattened out in the shape of a disc, and also $m_b$ and $m_a$ represent the mass of an incident droplet and splashed droplets respectively. In the above equation, $V_b$ and $V_a$ are the total velocity of an incident droplet and splashed droplets, respectively. Also, $t_e$ represents the life time of an incident droplet. The last term in the left-hand side represents the viscous dissipated energy and can be expressed as follows:

$$\int_0^{t_e} \int_{\forall_f} \varPhi d \forall_f dt \approx \mu_d (v_{bn}/\delta_f)^2 \pi d_{sp}^2 \delta_f t_e/4 \qquad (13)$$

where $d_{sp}$ and $\delta_f$ are the diameter and height of the film disc respectively. The main difference between the present model and earlier published models is in the determination of the total velocity of droplets after impingement by using the newly modeled relationship for the dissipated energy instead of the critical Weber number from the experimental data. Introducing the $\gamma_{max}$, $We_a{}^T$ and $We_b{}^T$ into Eq. (12), the following relation is obtained for the total velocity of ejected droplets:

$$We_a{}^T = \frac{C_w We_b{}^T}{r_m} - \left( \frac{K_v C_w We_{bn} \gamma_{max}{}^4}{r_m Re_{bn}} - \frac{12 C_w}{r_m} \right) - 12 \qquad (14)$$

where, $K_v$ is constant value of 4.5 and $\gamma_{max}$ is defined as $d_{sp,max}/D_b$ which is the dimensionless parameter of the disc when the splash occurs. Also, $We_a{}^T$ and $We_b{}^T$ are Weber numbers based on the total velocity of the splashing and impinging droplet, respectively. We assume that the splash occurs at the moment of crown emergence and, therefore, adopt $\gamma_{max}$ as 2.0 from the observation of Yarin and Weiss (1995). The second term in the right-hand side represents the dissipated energy of the droplet when the incident droplets impinge on the wall.

The next step is to determine the velocity components of ejected droplets. In the new model, we should determine the tangential component of the ejected droplets and then, from Eq. (14), the normal velocity and ejection angle of ejected droplets can be subsequently determined. Assuming that the tangential component of the droplet velocity after impingement can be approximated by the tangential velocity of the crown, a liquid sheet virtually normal to the wall, the position of the crown for a single-droplet impingement can be given from the theoretical relationship of Yarin and Weiss (1995) as follows:

$$\frac{r_c}{D_b} = \left( \frac{2}{3} \right)^{0.25} \frac{v_{bn}^{1/2}}{D_b^{1/4} \delta_f^{1/4}} (t - t_o)^{1/2} \qquad (15)$$

where $r_c$ and $t_o$ are the crown radius and the time for a droplet to create the initial spot in the center of the film, respectively. Finally, we can obtain the tangential velocity of ejected droplets from the above equation as follows:

$$v_f = 0.452 K_f \cdot Re_{bn}^{1/8} \cdot v_{bn}/\sqrt{\varPsi} \qquad (16)$$

where $\varPsi$ represents the time fraction which is defined as the ratio of time when the splash occurs to the residence time of an incident droplet. In a physical sense, this time fraction may be affected by the kinematic parameter of an incident droplet. Therefore, in the present study, the time fraction is derived as a function of the droplet Reynolds number.

$$\varPsi = 1.0 \quad \text{for } Re_{bn} \le 577 \qquad (17a)$$
$$\varPsi = 0.204 Re_{bn}^{0.25} \quad \text{for } Re_{bn} > 577 \qquad (17b)$$

According to Yarin and Weiss (1995), the theoretical relationship consistently overestimates the

experimental results due to their exclusion of the momentum losses at the moment of impingement. To consider the effect of viscosity, we introduce the friction factor, $K_f$, which is randomly chosen in the range between 0.81 and 0.91. This range is determined from the experimental consideration of Yarin and Weiss(1995). Hence, the tangential and normal components of ejected droplet velocity are given by using Eqs. (14) and (16). For three-dimensional calculations, it is necessary to determine the deflection angle $\omega$. We can finally obtain the tangential component of ejected droplet velocities as follows:

$$v_{at,x} = v_{bt,x} + v_f \cos \omega \qquad (18a)$$
$$v_{at,y} = v_{bt,y} + v_f \sin \omega \qquad (18b)$$

where, $\omega$ is chosen stochastically by using the correlation proposed by Naber and Reitz(1988). Subscripts x and y denote the components of tangential velocity in the cartesian coordinate.

## 3. Numerical Method

The gas phase is derived in terms of the Eulerian conservation equations and turbulent transport is modeled by the modified k-$\varepsilon$ model of Reynolds(1980). To couple the gas phase velocity with the pressure field, the implicit and non-iterative PISO algorithm is used in the present study. The gas phase transport equations are discretised by the finite volume method. With this process, the Euler implicit method is used for the transient term, and a hybrid upwind/central difference scheme is used to approximate the convection and diffusion terms. The droplet parcel equations of trajectory, momentum, mass and energy are written in Lagrangian form. The ordinary differential Lagrangian equations for the droplets are also discretised in the Euler implicit manner. Droplets may become unstable under the action of the interfacial forces induced by their motion relative to the continuous phase. The present study incorporates a breakup model widely used for the breakup of liquid droplets in a gaseous stream proposed by Reitz and Diwakar(1987), where two breakup regimes are identified as the bag and stripping breakup. Also, the collision and coales-

cence model of O'Rourke(1981) is used in this paper.

## 4. Results and Discussion

In the present work, numerical simulations are performed using the new model for validation. The computational domain for all cases with $50 \times 50 \times 40$ (x, y and z respectively) grids is used as shown in Fig. 1. The present resolution was found to give adequately grid-independent results performed by Lee et al. (1999). Table 1 presents the specifications of test cases performed in the present calculation. The cases 1 and 2 show the experimental conditions which have been used by Katsura et al. (1989). Also, the cases 3 and 4 show the specifications of Fujimoto et al. (1990)
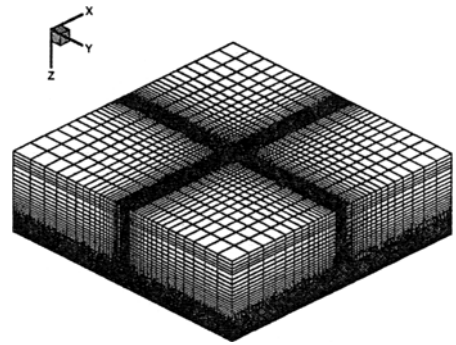


**Fig. 1** Grid generation

**Table 1** Test cases

| Cases | Case 1 | Case 2 | Case 3 | Case 4 | Case 5 |
|---|---|---|---|---|---|
| Wall Distance [mm] | 24 | 34 | 24 | 25 | 30 |
| Gas Pressure [bar] | 15 | 15 | 15 | 2 | 1 |
| Injection Pressure [bar] | 140 | 140 | 138 | 300 | 260 |
| Nozzle Diameter [mm] | 0.3 | 0.3 | 0.2 | 0.25 | 0.22 |
| Injection Duration [ms] | 1.2 | 1.2 | 1.3 | 2.85 | 1.0 |

and Saito et al. (1993), respectively. These condi-
tions were used to simulate the overall structure
of the non-evaporative impinging sprays. In par-
ticular, the numerical simulation for the case 5
was performed in order to analyze the internal
structure of wall sprays such as the local droplet
velocity, SMD (Sauter Mean Diameter) and the
mean velocity of the gas phase flow. The results
were compared with the experimental data of
Arcoumanis and Chang (1994).

For all cases, a time step 10 $\mu$s is adopted and
in the case 1, a total of 4000 drop parcels is
introduced through injection duration time. The
computing time for convergence is about 2.4 hr
for the case 5 using CRAYC90. For the cases 1 to
4, we used the model by Reitz and Diwakar
(1987) to describe the breakup process of liquid
jets at the nozzle exit. Reitz (1987) applied the
wave stability atomization theory to diesel spray
modeling, by injecting parcels of liquid in the
form of "blobs" that had a characteristic size
equal to the nozzle hole diameter, instead of
assuming an intact liquid at the nozzle exit. The
basis of this model is the concept introduced by
Reitz and Diwakar (1987) that atomization of the
injected liquid and the subsequent breakup of
droplets are indistinguishable processes within
dense spray. According to Reitz and Diwakar
(1987), however, the above model may cause the
impinging droplet size to be exaggerated for
impinging sprays with the low gas density like the
case 5. Hence, we assumed that the initial size of
droplets could be determined by using a Gaussian
distribution with the mean diameter of 40 $\mu$m.
This value is given from the experimental results,
in which the SMD at the centerline of the free
spray at 30 mm distance from the nozzle exit is
about 40 $\mu$m because there is no relevant informa-
tion in the experimental conditions about the
initial droplet size distribution.

The schedules of injection velocity for the cases
1, 2 and 5 were determined by the curve-fitted
relationship from the experimental data produced
by Katsura et al. (1989) and Arcoumanis and
Chang (1994). However, the velocity schedules
for the cases 3 and 4 were assumed by constant
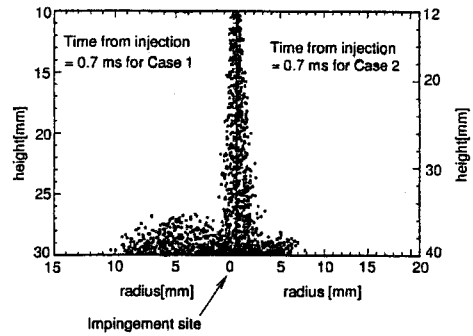velocity based on the experimental condition



Fig. 2  The predicted spray patterns for cases 1 and 2

because it could not be found from the related
references of Fujimoto et al. (1990) and Saito et
al. (1993).

### 4.1  Overall structure of wall spray

To begin with, we analyze the overall structure
of wall spray for high gas density in cases 1 to 4.
The main parameters which represent the overall
structure of wall sprays are the radius and height
of wall spray. For the cases 1 and 2, Katsura et al.
(1989) conducted the experiments in which a
single spray was normally impinged on a flat
plate at high trap pressure and room temperature.
Figure 2 shows the predicted spray patterns for
the cases 1 and 2 at 0.7 ms. The spray radius
decreases as the impingement distance increases,
indicating that a longer time is needed for the
spray to reach the wall prior to impingement.
Figure 3 compares the calculated wall spray
radius and height with the experimental data of
Katsura et al. (1989) for the cases 1 and 2. The
spray height results show good agreements with
maximum error 7.6 % for the case 1 and 1.6 % for
the case 2, suggesting that the current model can
effectively predict the behavior of splashing dro-
plets. It can be observed that at the early stage
after start of impingement, the spray radius results
are in good agreement with the experimental data.
However, the present model under-predicts the
spray radius at the later stage of injection. Maxi-
mum error is about 12.1 % and 11.6 % for the case
1 and the case 2, respectively, at the end of the
total calculation time. This discrepancy is larger
toward the end of the injection duration, and
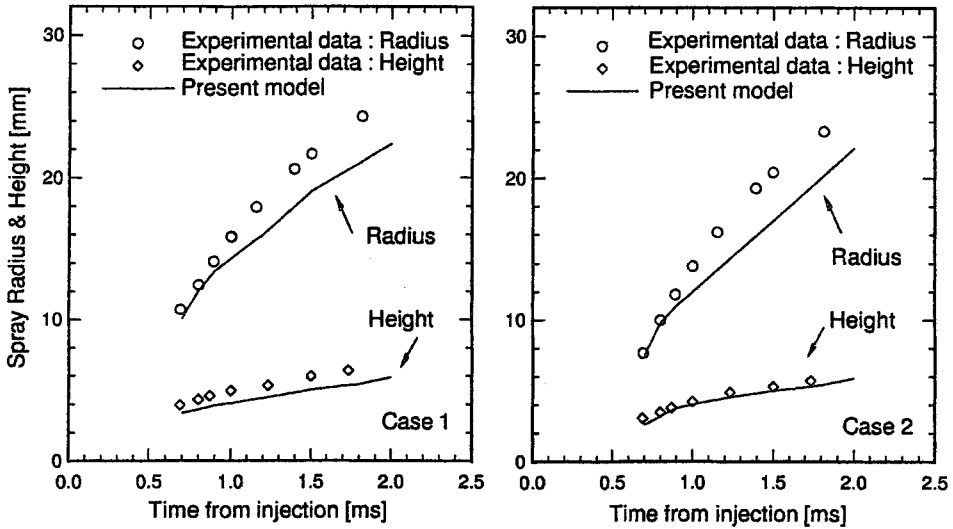caused by modeling of the droplet size distribu-

Fig. 3   Comparison of spray radius and height with experimental data (Cases 1 and 2)
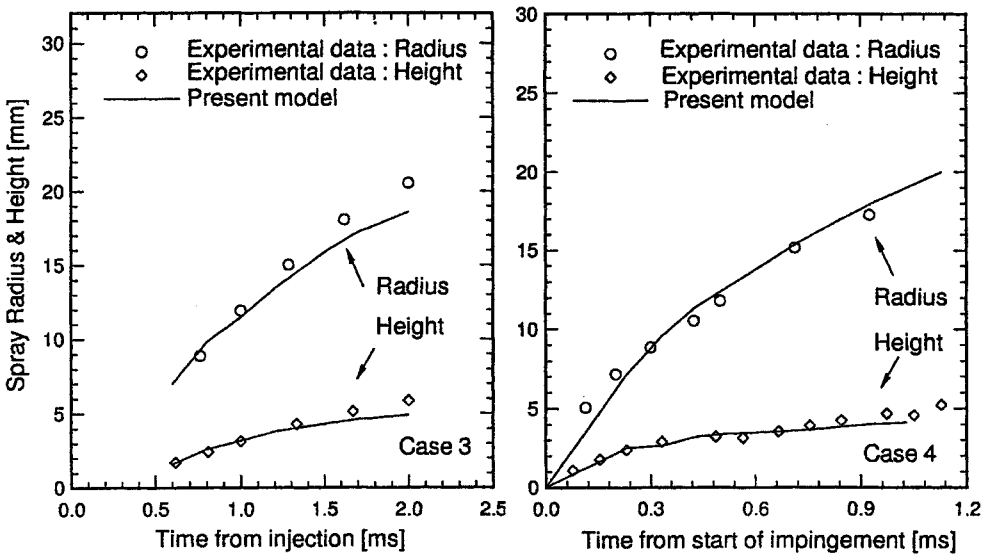


Fig. 4   Comparison of spray radius and height with experimental data (Cases 3 and 4)

tion after impingement. The distribution being involved in the new model is based on the experimental data of Naber and Farrell(1993). For the very high Weber number, this distribution may produce smaller droplets than those in the actual phenomena. In this case, smaller droplets ejected due to the impingement can not penetrate in the radial direction effectively because of insufficient inertia of ejected droplets. Therefore, it is thought that more accurate experimental data for the size distribution of ejected droplets are required in order to produce better prediction.

Figure 4 represents the comparison of spray radius and height with the experimental data of Fujimoto et al. (1990) for the case 3 and Saito et al. (1993) for the case 4. It can be seen in the case 3 that the present model predicts the similar trend with the experimental data for spray radius, although the radius of wall spray is slightly under -predicted with maximum error of 9.5 % at 2.0 ms. Meanwhile, the present prediction gives excellent agreement with the experimental data for the

spray height. For the case 4, very good agreement is observed for the wall spray radius and height, indicating that the transient behavior of wall sprays can be effectively predicted by the present model.

### 4.2  Internal structure of wall spray

During the last decade, most sub-models for numerical calculation have been assessed by comparing the overall structure with the experimental data. However, it is important to analyze the internal structure of wall sprays to give better understanding of the interaction between the gas-phase flow and the dispersed droplets because the internal structure affects the heat transfer rate and transient behavior of ejected droplets in the real DI engines and consequently influences the overall structure. In addition, the examination of internal structure will help account for assessment of the impingement model and for transient behavior of wall sprays more effectively. The main parameters of internal structure are such as the local droplet velocities, SMD and velocities of the gas-phase flow.

The new model results are compared with the experimental data of Arcoumanis and Chang (1994). Figure 5 shows the measuring locations, corresponding to representative regions of the two-phase wall-jet, referred by Kasura et al. (1989), such as the main wall-jet region(1), the stagnation region(2) and the downstream region(3). Figures 6 and 7 represent the comparison of the calculated tangential velocities of droplets at the main wall-jet region(r=6mm, H=0.5mm) and near the stagnation region(r=10mm, H=5.0mm). The present model gives the exaggerated

prediction of drop tangential velocity around the early stage of impingement, but produces the prediction of the similar trend as time goes on. These figures show that the tangential velocity starts at a maximum velocity and then gradually decays to approximately zero. Near-wall velocities are not settled to a quasi-steady state within the whole injection duration, but those in the stagnation region are settled to it. Additionally, the mean velocity decreases as the distance from the wall surface increases, suggesting that most of the droplet tangential momentum remains concentrated near the wall surface. This trend is in good agreement with the experimental consideration of Arcoumanis and Chang(1994). However, in contrast with the experimental observation, the actual spray are reached to a quasi-steady state slightly earlier than that predicted by the present model. Figures 8 and 9 show the SMD profiles in the
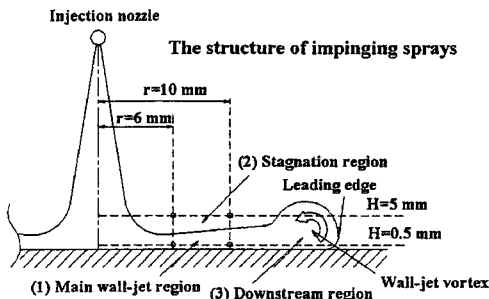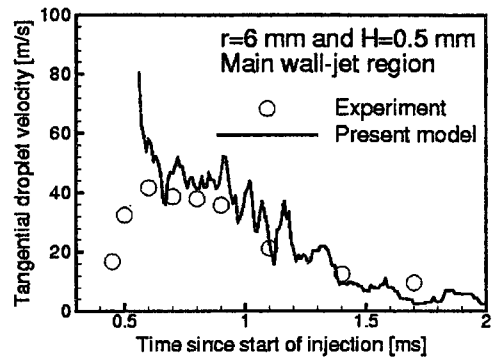


**Fig. 6**  The tangential droplet velocity at r=6 mm and H=0.5 mm
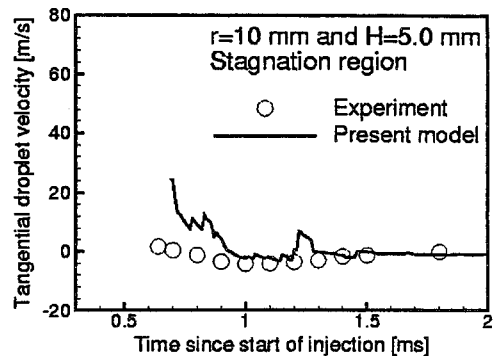


**Fig. 7**  The tangential droplet velocity at r=10 mm and H=5.0 mm



**Fig. 5**  Measuring locations (Case 5)
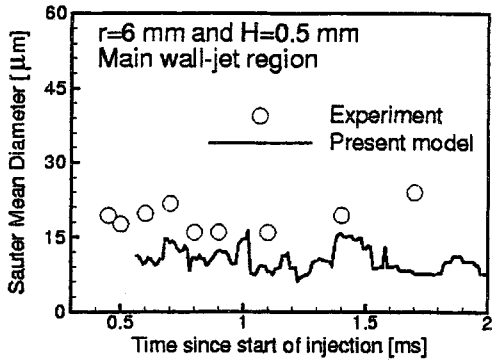
Fig. 8   The SMD profiles at r=6 mm and
         H=0.5 mm



Fig. 9   The SMD profiles at r=10 mm and
         H=5.0 mm



Fig. 10   The normal component of the gas-phase
          velocity at r=10mm and H=3.0mm



Fig. 11   The tangential component of the gas-phase
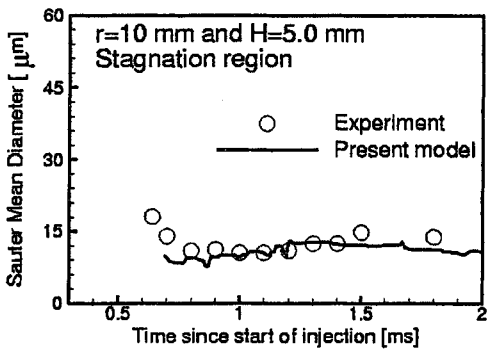          velocity at r=10mm and H=3.0mm

main wall jet and the stagnation regions. The new model under-predicts the SMD values at the main wall-jet region. This may be partly due to the breakup and coalescence model near the wall and partly due to the inappropriate size distribution of droplets after impingement. It is, however, found that the predicted SMDs near the stagnation region are generally in good agreement with the experimental data except for those at the first stage of injection. This indicates that the coalescence model used in the paper performs better in the stagnation region that is far away from the wall, relative to the near-wall region. Therefore, it might be thought that the appropriate model for droplet coalescence should be considered near the wall to produce more accurate predictions of SMDs.

Figures 10 and 11 compare the magnitude of the normal and tangential velocities of the gas-phase flow near stagnation region. In Fig. 10, the
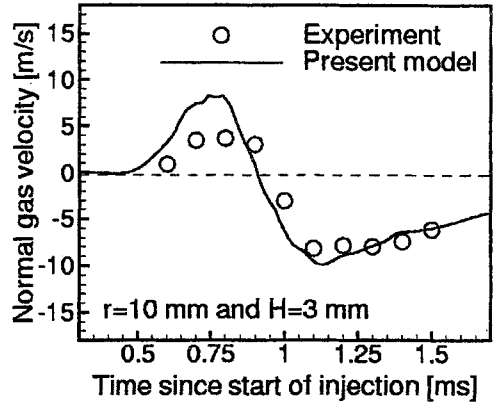
positive direction of the normal velocity is defined as the direction away from the wall. According to Arcoumanis and Chang(1994), the center of the vortical structure can be determined by the position where the normal velocity is zero which allows the arrival time of the vortex center at a certain position in question to be estimated by identifying the time at which the normal velocity crosses the zero line. The predicted time changing the velocity magnitude to a negative value is in good agreement with the experimental data. It becomes clear from Fig. 10 that the new model is capable of predicting the temporal behavior of the head vortex resulting from impinging sprays. Since the region of negative velocities indicates that the surrounding gas is entrained into the main wall-jet region, it is seen

from Fig. 10 that the present model is acceptable for the prediction of the magnitude of the entrained surrounding gas into the main wall-jet region.

As shown in Fig. 11, although there are some discrepancies at early stage of injection, the prediction of tangential velocities is good after 0.9 ms, compared with the experimental data. As time goes on, the predicted tangential velocities reach to the quasi-steady state of positive value. Actually, the occurrence of minimum of the normal and tangential velocities at a certain time indicates that the head vortex passes through a point in question at that time. Through Figs. 10 and 11, the present model shows that the time at which the head vortex passes through is about 0.85 to 0. 9 ms, indicating that the present model effectively predicts the temporal behavior of head vortex.

## 5. Conclusions

A new sub-model for spray/wall impingement was developed and tested against the several experimental data. The new model was basically devised to be capable of describing the situations involving wall temperatures below the fuel boiling temperature. The main feature of the new model is in determination of the tangential and normal velocities after impingement. The newly derived formulae for the dissipated energy of the film and the tangential film velocity was introduced in the present study. The following conclusions can be drawn.

**A. Overall structure of wall sprays**: For the cases 1, 2 and 3, the new model comparatively showed the good prediction of the wall spray height, compared to the experimental data. However, there were some discrepancies in predicting the radial penetration of wall sprays. In particular, in the case 4, the calculated radius and height of wall sprays were in good agreement with the experimental data.

**B. Internal structure of wall sprays**: The new model could effectively predict the qualitative characteristics of wall sprays, local droplet velocity, SMD and local gas velocities. The predictions for the tangential velocities and SMDs of secon-

dary droplets were in good agreement with the experimental data.

Therefore, it can be concluded that the present model is useful in predicting the transient behavior of diesel sprays impinging on a wall. Nevertheless, there is a clear need for more elaborated model which can predict all aspects of droplet impingement. Therefore, the present model will be modified and tested continuously to obtain the more accurate predictions.

## References

Arcoumanis C. and Chang, J. C., 1994, "Flow and Heat Transfer Characteristics of Impinging Transient Diesel Sprays," *SAE940678*.

Bai, C and Gosman, A. D., 1995, "Development of Methodology for Spray Impingement Simulation," *SAE950283*.

Eckhause, J. E. and Reitz, R. D., 1995, "Modeling Heat Transfer to Impinging Fuel Sprays in Direct-Injection Engines," *Atomization and Sprays*, Vol 5, pp. 213~242.

Fujimoto, H., Senda, J., Nagae, M., Hashimoto, A., Saito, M. and Katsura, N., 1990, "Characteristics of a Diesel Spray Impinging on a Flat Wall," *COMODIA 90 Proceedings of International Symposium on Diagnostics and Modeling of Combustion in Internal Combustion Engines*, pp. 193~198, Kyoto, Japan.

Gonzalez, M. A., Borman, G. L. and Reitz, R. D., 1991, "A Study of Diesel Cold Starting Using Both Cycle Analysis and Multidimensional Calculations," *SAE910180*.

Guerrassi, N. and Champoussin, J. C., 1996, "Experimental Study and Modeling of Diesel Spray/Wall Impingement," *SAE960864*.

Katsura, N., Saito, M., Senda, J. and Fujimoto, H., 1989, "Characteristics of a Diesel Spray Impinging on a Flat Wall," *SAE890264*.

Kolpakov, A. V., Romanov, K. V. and Titova, E. I., 1985, "Calculation of the Rebound Condition for Colliding Drops of Sharply Different Sizes," *Kolloidn. Zh.*, Vol. 47, p. 953.

Lee, S. H., Ryou, H. S., and Chae, S., 1999, "Development of a New Spray/Wall Interaction Model," *2nd International Symposium on Two-*

*Phase Flow Modeling and Experimentation*, Vol. 3, pp. 1915~1999, Pisa, Italy, 23-26.

Matsumoto, S. and Saito, S., 1970, "On the Mechanism of Suspension of Particles in Horizontal Conveying : Monte Carlo Simulation Based on the Irregular Bouncing Model," *J. Chem. Engng. Japan*, Vol. 3, pp. 83~92.

Mundo, C., Sommerfeld, M. and Tropea, C., 1995, "Droplet-Wall Collisions : Experimental Studies of the Deformation and Breakup Process," *Int. J. Multiphase Flow*, Vol. 21, pp. 151~173.

Mundo, C, Sommerfeld, M. and Tropea, C., 1998, "On the Modeling of Liquid Sprays Impinging on Surfaces," *Atomization and Sprays*, Vol. 8, pp. 625~652.

Naber, J. D. and Farrell, P., 1993, "Hydrodynamics of Droplet Impingement on a Heated Surface," *SAE930919*.

Naber, J. D. and Reitz, R. D., 1988, "Modeling Engine Spray/Wall Impingement," *SAE880107*.

O'Rourke, P. J., 1981, *Collective Drop Effects on Vaporizing Liquid Sprays*, Ph. D Thesis of Princeton Univ.

Park, K., 1994, *Development of a Non-Orthogonal-Grid Computer Code for the Optimization of Direct-Injection Diesel Engine Combustion Chamber Shapes*, Ph. D. Thesis, UMIST, UK.

Reitz, R. D., 1987, "Modeling Atomization Processes in High-Pressure Vaporizing Sprays," *Atomization and Spray Technology*, Vol. 3, pp. 309~337.

Reitz, R. D. and Diwakar, R., 1987, "Structure of High-Pressure Fuel Sprays," *SAE870598*.

Reynolds, W. C., 1980, *Modeling of Fluid Motions in Engines-an Introductory Overview, in Combustion Modeling in Reciprocating Engines*, ed. J. N. Mattavi and C. A. Amann, Plenum Press, NY.

Saito, A., Kawamura, K., Watanabe, S., Takahashi, T. and Tuzuki, N., 1993, "Analysis of Impinging Spray Characteristics under High-Pressure Fuel Injection (1st Report, Measurements of Impinging Spray Characteristics)," *Trans. of Jap. Soc. Mech. Engg.*, Part. B, Vol. 59, pp. 3290~3295.

Senda, J., Kanda, T., Al-Roub, M., Farrell, P. V., Fukami, T. and Fujimoto, H., 1997, "Modeling Spray Impingement Considering Fuel Film Formation on the Wall," *SAE970047*.

Stanton, D. W. and Rutland, C. J., 1996, "Modeling Fuel Film Formation and Wall Interaction in Diesel Engines," *SAE960628*.

Watkins, A. P. and Wang, D. M., 1990, "A New Model for Diesel Spray Impaction on Walls and Comparison with Experiment," *COMODIA 90 Proceedings of International Symposium on Diagnostics and Modeling of Combustion in Internal Combustion Engines*, pp. 243~248, Kyoto, Japan.

Wachters, L. H. J and Westerling, N. A. J., 1966, "The Heat Transfer From a Hot Wall to Impinging Water Drops in a Spherical State," *Chem. Eng. Sci.*, Vol. 21, pp. 1047~1056.

Yarin, A. L. and Weiss, D. A., 1995, "Impact of Drops on Solid Surfaces : Self-Similar Capillary Waves, and Splashing as a New Type of Kinematic Discontinuity," *J. Fluid Mech.*, Vol. 283, pp. 141~173.